

# Electronic Detection of the Enzymatic Degradation of Starch

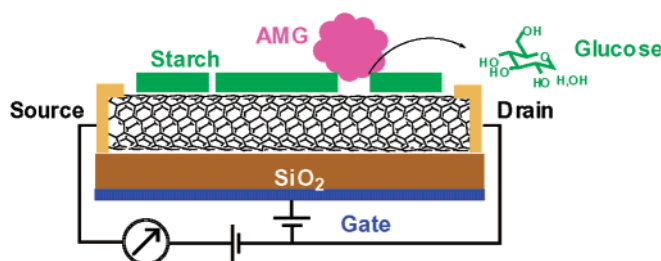
Alexander Star,<sup>\*,†</sup> Vikram Joshi,<sup>†</sup> Tzong-Ru Han,<sup>†</sup> M. Virginia P. Altoé,<sup>†</sup>  
George Grüner,<sup>†,‡</sup> and J. Fraser Stoddart<sup>§</sup>

Nanomix, Inc., 5980 Horton Street, Suite 600, Emeryville, California 94608,  
and Department of Physics and Astronomy, and California NanoSystems Institute and  
Department of Chemistry and Biochemistry, University of California,  
Los Angeles, California 90095

astar@nano.com

Received March 6, 2004

## ABSTRACT



The enzymatic degradation of starch can be monitored electronically using single-walled carbon nanotubes (SWNTs) as semiconducting probes in field-effect transistors (FETs). Incubation of these devices in aqueous buffer solutions of amyloglucosidase (AMG) results in the removal of the starch from both the silicon surfaces and the side walls of the SWNTs in the FETs, as evidenced by direct imaging and electronic measurements.

The polysaccharide starch, which is composed of a linear (amylose) glucan and a branched (amylopectin) one, can be biodegraded<sup>1</sup> by microorganisms, such as fungi and bacteria, that are able to adapt to new substrates and produce a wide range of enzymes. With the virtuous goal of reducing environmental contamination, starch has been introduced into composite materials as a filler in order to increase the rates of degradation of selected synthetic polymers. There have already been several investigations<sup>2</sup> on the biodegradation of composite materials in which starch has been incorporated into a polymeric matrix, e.g., polyethylene, polycaprolactone, and poly(vinyl alcohol). The monitoring of the enzymatic degradation of starch-polymer composites was carried out

using tapping-mode atomic force microscopy (AFM) in order to ascertain the surface properties of the film.

Recently, we described<sup>3</sup> the preparation of starch composites with single-walled carbon nanotubes (SWNTs). The

(2) (a) Wool, R. P.; Raghavan, D.; Wagner, G. C.; Billieux, S. *J. Appl. Polym. Sci.* **2000**, *77*, 1643–1657. (b) Moreno-Chulim, M. V.; Barahona-Perez, F.; Canche-Escamilla, G. *J. Appl. Polym. Sci.* **2003**, *89*, 2764–2770.

(3) (a) Star, A.; Steuerman, D. W.; Heath, J. R.; Stoddart, J. F. *Angew. Chem., Int. Ed.* **2002**, *41*, 2508–2512. About the time this paper appeared, it was reported that aqueous solutions of the acidic polysaccharide, gum arabic, produced by Acacia Senegal trees, assists in the dispersal of SWNTs in water. See: (b) Bandyopadhyaya, R.; Nativ-Roth, E.; Regev, O.; Yerushalmi-Rozen, R. *Nano Lett.* **2002**, *2*, 25–28. Subsequently, it was shown the SWNTs can be solubilized simply and efficiently with amylose in aqueous dimethyl sulfoxide: the best solvent ratio is one that contains 10–20% dimethyl sulfoxide. See: (c) Kim, O.-K.; Je, J.; Baldwin, J. W.; Kooi, S.; Pehrsson, P. E.; Buckkey, L. J. *J. Am. Chem. Soc.* **2003**, *125*, 4426–4427. Very recently, it has been shown that both curdlan and schizophyllan ( $\beta$ -1,3-glucans) can entrap SWNTs in their helical superstructures. See: (d) Numata, M.; Asai, M.; Kaneko, K.; Hasegawa, T.; Fujita, N.; Kitada, Y.; Sakurai, K.; Shinkai, S. *Chem. Lett.* **2004**, *33*, 232–233.

<sup>†</sup> Nanomix, Inc.

<sup>‡</sup> Department of Physics and Astronomy.

<sup>§</sup> California NanoSystems Institute and Department of Chemistry and Biochemistry.

(1) Schnabel, W. *Polymer Degradation*; Henser International: Berlin, 1981; Chapter 6.

composites can be obtained by solubilizing SWNTs in aqueous solutions of starch. The composites have been investigated in aqueous solution by spectroscopic means and on surfaces using an AFM. We have also observed<sup>3</sup> that the enzymatic degradation of starch, in these water-soluble composites, is efficient at precipitating SWNTs wrapped with starch from their aqueous solutions. In this paper, we describe how the enzymatic degradation of starch can be monitored by direct imaging and electronic measurements, using SWNTs as semiconducting probes.

Starch consists<sup>4</sup> of a linear component—namely amylose—which is composed of  $\alpha$ -1,4 linkages between D-glucopyranose residues and a branched one—namely amylopectin—which, in addition to containing  $\alpha$ -1,4 linked chains of D-glucopyranose residues, carries branch points at the C-6 position on every 25 or so residues. Once again, the 1,6-linkages have the  $\alpha$ -configuration. The overall structure of amylopectin is dendritic in nature. The chains of  $\alpha$ -1,4 linked D-glucopyranose residues in amylose and amylopectin have a tendency to be helical, particularly in the presence of suitable guest ions or molecules. We have examined the enzymatic hydrolysis<sup>5</sup> of starch (Scheme 1) with amyloglucosidase (AMG) in acidic buffer solutions and noted that it results in complete cleavage of the polysaccharide chains down to water-soluble glucose. Furthermore, we have employed AFM to follow the breakdown of starch<sup>6</sup> by AMG on a silicon surface. This approach has made it possible for us to have direct visual evidence<sup>7</sup> for the presence or absence of starch during the enzymatic process.

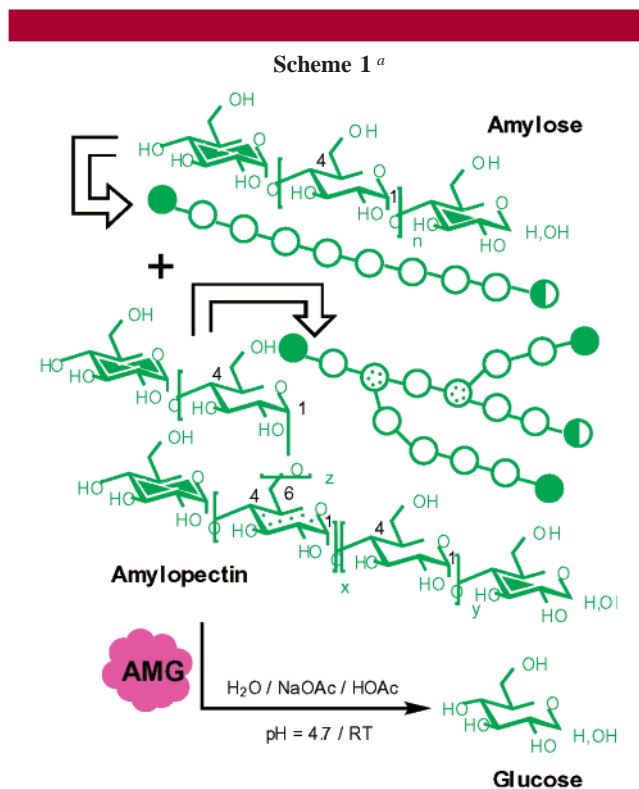
Figure 1 portrays AFM images obtained after depositions of starch on a clean silicon wafer and after exposure to a 0.1 M buffered solution of AMG. Starch deposition, carried out by incubating the clean silicon wafer in a 5% aqueous starch solution, leaves, after thorough rinsing with H<sub>2</sub>O, uneven deposits (see inside the circles in Figure 1a) which range from 30 to 100 nm in diameter. Applying the aqueous buffer solution alone leaves the starch-like topography intact (see inside the circles in Figure 1b), indicating that the buffer

(4) (a) Collins, P.; Ferrier, R. *Polysaccharides: Their Chemistry*; John Wiley & Sons: Chichester, 1995; pp 478–523. (b) Lehmann, J. *Carbohydrates: Structure and Biology*; Georg Thieme Verlag: Stuttgart, 1998; pp 98–103. (c) Thompson, D. B. *Carbohydr. Polym.* **2000**, *43*, 223–239.

(5) Among the numerous enzymes that will hydrolyze starch, there is amyloglucosidase, an exoamylase which attacks all the  $\alpha$ -1,4 and  $\alpha$ -1,6 glucosidic linkages to produce glucose. For more information about the properties of this and other glucosidases, see: Yamamoto, T. *Enzyme Chemistry and Molecular Biology of Amylases and Related Enzymes*; CRC Press, Inc.: Boca Raton, 1995; pp 3–201.  $\alpha$ -Amylase, which is present in human saliva, is an endoamylase which attacks the  $\alpha$ -1,4 glucosidic linkages in starch randomly and so reduces the lengths of the glucan chains drastically.

(6) Sample preparation for AFM was accomplished by first treating a silicon wafer in a piranha (H<sub>2</sub>O<sub>2</sub>, H<sub>2</sub>SO<sub>4</sub>) bath. The wafer was then incubated in a starch solution (5 wt % in H<sub>2</sub>O) for 30 min. After soaking, the wafer was thoroughly rinsed with H<sub>2</sub>O. The topographical data were recorded with a Digital Instruments Multimode AFM equipped with a high-resolution stage and controlled by a Nanoscope IIIa scanning probe microscope controller with a Nanoscope Extender. The images were taken with standard tips in tapping mode at a scan rate of 1.5 Hz.

(7) The enzymatic degradation of starch was performed as follows. The amyloglucosidase was prepared at a concentration of 50 mg in 1 mL of a 4.5 pH buffer solution consisting of 0.1 M NaOAc and 0.1 M HOAc. The starch-coated wafers were placed in the enzyme solution for 24 h before being rinsed with H<sub>2</sub>O. Specifically, the wafers were suspended vertically in solution to avoid nonspecific precipitation.



<sup>a</sup> The enzyme, amyloglucosidase (AMG), hydrolyzes starch, a mixture of amylose (the linear component) and amylopectin (the branched component), from the nonreducing end (shaded) of the D-glucans which contain  $\alpha$ -1,4 linkages (amylose) and  $\alpha$ -1,6 as well as  $\alpha$ -1,4 linkages (amylopectin) in a 0.1 M sodium acetate buffer at pH 4.7 at room temperature.

without the enzyme is incapable of removing the starch from the surface of silicon. By comparison, however, AFM imaging (Figure 1c) shows that most of the physical indications of starch deposition are removed after incubation with AMG for 1 day. Thus, the enzyme is effective in either breaking down or changing the starch such that it is removed from the surface of the silicon. At the same time, the enzyme produces its own particular characteristic deposit in the form of granule-like particles (Figure 1c). Deposition of AMG on clean silicon wafers resulted in surface features similar to those shown in this figure. AMG used in the study contained a significant percentage of diatomaceous earth<sup>8</sup> and it may be responsible for these surface deposits.

The deposition<sup>9</sup> of starch on SWNTs was also investigated by transmission electron microscopy (TEM). Starch was deposited by drop casting of a 1% starch solution in H<sub>2</sub>O

(8) Diatomaceous earth—a substance made up from crushed fossils of freshwater organisms and marine life—is an additive to amyloglucosidase from *Rhizopus* sp. (Sigma).

(9) The preparation of starch-coated SWNTs for TEM was carried out as follows: The CVD grown carbon nanotubes were removed from the surface of a 100 mm silicon wafer by ultrasonication of several small pieces in 1,2-dichlorobenzene for 5 min. Drops of the nanotube suspension were dispersed onto a lacey carbon film 300 mesh copper TEM grid. One drop of a 1% starch water solution was placed on the surface of the TEM grid with nanotubes for 1 min, followed by rinsing in pure H<sub>2</sub>O and drying in air. In a final step, the TEM grid was exposed to RuO<sub>4</sub> vapor for 1 min. High-resolution TEM (HRTEM) images were obtained using a 002B-TOPCON microscope at 120 kV in the National Center for Electron Microscopy at the Lawrence Berkeley National Laboratory.

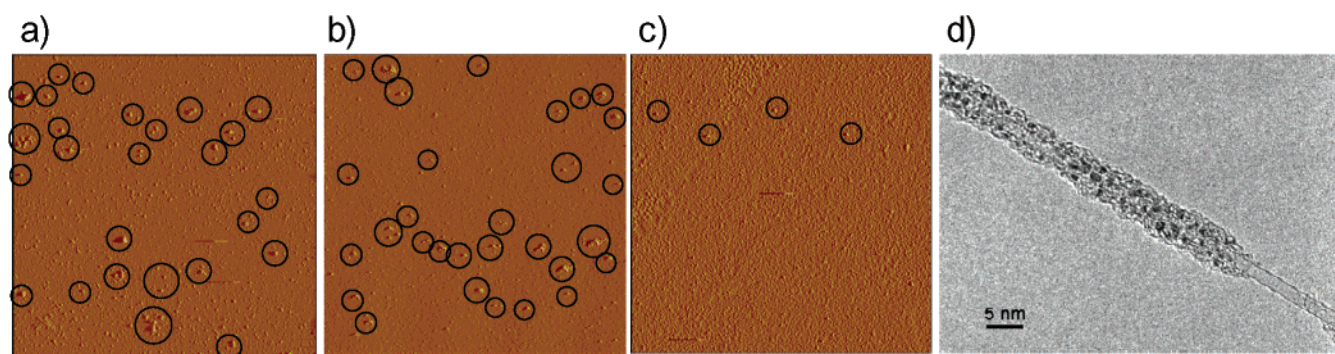


**Figure 1.** AFM images (tapping mode,  $5 \times 5 \mu\text{m}$ ) of starch dip-coated on a cleaned, plain Si wafer (a) directly from a 5% aqueous solution, (b) after treatment of the Si wafer with a 0.1 M sodium acetate buffer, and (c) after treatment of the Si-wafer with AMG (concentrated of 50 mg in 1 mL) in the buffer solution. Circles indicate areas on the wafer where large aggregates of starch molecules reside. (d) High-resolution transmission electron microscopy (HRTEM) image of a SWNT (2.0 nm diameter) on a lacey carbon film 300 mesh copper TEM grid after treatment with a drop of a 1% of an aqueous solution of starch. The starch has been stained with  $\text{RuO}_4$  vapor.

on a TEM grid containing SWNTs. For imaging purposes, the starch was contrasted by a  $\text{RuO}_4$ -staining procedure.<sup>10</sup> Figure 1d illustrates a high-resolution electron transmission microscopy (HRTEM) image of a SWNT of diameter of 2 nm, covered with starch: substantial coverage of the nanotube with the amorphous polysaccharide is evident. The dark spots on the image are the ruthenium atoms attached to the amorphous polysaccharide (lighter color). On the side-wall of the SWNT where there is no starch, no ruthenium staining is observed either.

We have also explored the electronic detection of the enzymatic hydrolysis of starch using SWNTs as semiconducting probes. Electronic devices,<sup>11</sup> based on field-effect transistors (FETs) incorporating carbon nanotubes as the semiconducting channel, have been investigated recently for the electronic detection of chemical,<sup>12</sup> as well as other biological,<sup>13</sup> functions.

(10) An  $\text{RuO}_4$  staining solution was prepared by adding  $\text{RuCl}_3 \cdot 3\text{H}_2\text{O}$  (20 mg) to a 10 wt % solution of sodium hypochlorite (1 mL) in an 8 mL vial. The mixture was immediately capped. The TEM grid was attached to the bottom of the vial cap to expose grid to the staining vapors. For the staining procedure, see: Brown, G. M.; Butler, J. H. *Polymer* **1997**, *38*, 3937–3945.

(11) For examples of the use of carbon nanotube FET devices, see: (a) Tans, S. J.; Verschuere, R. M.; Dekker, C. *Nature* **1998**, *393*, 49–52. (b) Martel, R.; Schmidt, T.; Shea, H. R.; Hertel, T.; Avouris, Ph. *Appl. Phys. Lett.* **1998**, *73*, 2447–2449. (c) Bachtold, A.; Hadley, P.; Nakanishi, T.; Dekker, C. *Science* **2001**, *294*, 1317–1320. (d) Kong, J.; Dai, H. *J. Phys. Chem. B* **2001**, *105*, 2890–2893. (e) Shim, M.; Javey, A.; Kam, N. W. S.; Dai, H. *J. Am. Chem. Soc.* **2001**, *123*, 11512–11513. (f) Derycke, V.; Martel, R.; Appenzeller, J.; Avouris, Ph. *Appl. Phys. Lett.* **2002**, *80*, 2773–2775. (g) Fuhrer, M. S.; Kim, B. M.; Dürkop, T.; Brintlinger, T. *Nano Lett.* **2002**, *2*, 755–759. (h) Radosavljevic, M.; Freitag, M.; Thadani, K. V.; Johnson, A. T. *Nano Lett.* **2002**, *2*, 761–764. (i) Bradley, K.; Cummings, J.; Star, A.; Gabriel, J.-C. P.; Grüner, G. *Nano Lett.* **2003**, *3*, 639–641. (j) Misewich, J. A.; Martel, R.; Avouris, Ph.; Tsang, J. C.; Heinze, S.; Tersoff, J. *Science* **2003**, *300*, 783–786. (k) Javey, A.; Guo, J.; Wang, Q.; Lundstrom, M.; Dai, H. *Nature* **2003**, *424*, 654–657.

(12) For examples of chemical sensing using carbon nanotubes, see: (a) Collins, P. G.; Bradley, K.; Ishigami, M.; Zettl, A. *Science* **2000**, *287*, 1801–1804. (b) Kong, J.; Franklin, N. R.; Zhou, C.; Chapline, M. G.; Peng, S.; Cho, K.; Dai, H. *Science* **2000**, *287*, 622–625. (c) Kong, J.; Chapline, M. G.; Dai, H. *Adv. Mater.* **2001**, *13*, 1384–1386. (d) Qi, P.; Vermesh, O.; Grecu, M.; Javey, A.; Wang, Q.; Dai, H.; Peng, S.; Cho, K. *J. Nano Lett.* **2003**, *3*, 347–351. (e) Star, A.; Han, T.-R.; Gabriel, J.-C. P.; Bradley, K.; Grüner, G. *Nano Lett.* **2003**, *3*, 1421–1423.

FET devices, incorporating carbon nanotubes, were fabricated<sup>14</sup> using SWNTs grown in situ by chemical vapor deposition (CVD) on 100 mm silicon wafers. Electrical contacts were patterned by standard optical lithography in order to fabricate thousands of devices on the wafer. The device architecture that was used in this study is displayed in Figure 2. In the devices which were fabricated, multiple nanotubes connect the source and drain electrodes with the electrical characteristics of individual tubes varying from metallic to semiconducting.<sup>15</sup> For the experiments reported here, devices dominated by semiconducting nanotube channels were selected using a wafer autoprober. These devices display (Figure 3a) transconductance and source-drain current–voltage characteristics, typical of the p-type device behavior caused by atmospheric oxygen on the side-wall of the nanotube.<sup>12a</sup> The device characteristics—i.e., the source-drain current  $I$  as a function of the gate voltage  $V_g$ , viz.,  $I/V_g$ —were measured in order to evaluate the effect of starch deposition and the subsequent enzymatic degradation of the starch layer on the carbon nanotubes. All the electronic measurements were performed in air after the buffer solution had been removed.

(13) For recent examples of biosensors based on carbon nanotube FETs, see: (a) Star, A.; Gabriel, J.-C. P.; Bradley, K.; Grüner, G. *Nano Lett.* **2003**, *3*, 459–463. (b) Chen, R. J.; Bangsaruntip, S.; Drouvalakis, K. A.; Wong Shi Kam, N.; Shim, M.; Li, Y.; Kim, W.; Utz, P. J.; Dai, H. *Proc. Natl. Acad. Sci. U.S.A.* **2003**, *100*, 4984–4989. (c) Besteman, K.; Lee, J.-O.; Wiertz, F. G. M.; Heering, H. A.; Dekker, C. *Nano Lett.* **2003**, *3*, 727–730. (d) Boussaad, S.; Tao, N. J.; Zhang, R.; Hopson, T.; Nagahara, L. A. *Chem. Commun.* **2003**, 1502–1503. (e) Bradley, K.; Briman, M.; Star, A.; Grüner, G. *Nano Lett.* **2004**, *4*, 253–256. (f) Chen, R. J.; Choi, H. C.; Bangsaruntip, S.; Yenilmez, E.; Tang, X.; Wang, Q.; Chang, Y.-L.; Dai, H. *J. Am. Chem. Soc.* **2004**, *126*, 1563–1568.

(14) NTFET devices were fabricated using SWNTs grown by chemical vapor deposition (CVD) on 200 nm of  $\text{SiO}_2$  on doped Si from Fe nanoparticles with  $\text{CH}_4/\text{H}_2$  gas mixture at 900 °C. Electrical leads were patterned on top of the nanotubes from Ti films 35 nm thick, capped with Au layers 5 nm thick, with a spacing of 0.75  $\mu\text{m}$  between the source and drain. The experimental details relating to the NTFET device fabrication have been published. See: Gabriel, J.-C. P. *Mater. Res. Soc. Symp. Proc.* **2003**, *776*, Q12.7.1–7.

(15) Electronic measurements on NTFET devices, such as current flow between S/D electrodes as function of applied gate voltage, were conducted using a semiconductor parameter analyzer (Keithley 4200).

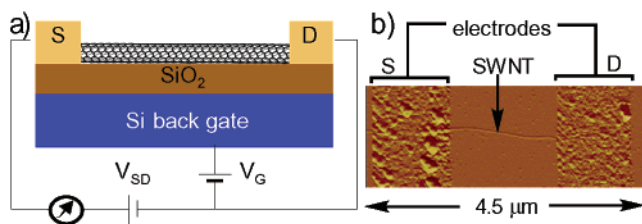


**Figure 2.** (a) Schematic representation of a nanotube field-effect transistor (NTFET) device with a semiconducting SWNT (black) contacted by two Ti/Au electrodes (light brown) representing the source (S) and the drain (D) with a Si back gate (dark blue) separated by a SiO<sub>2</sub> insulating layer (dark brown) in a transistor-configured circuit. (b) AFM Image of a typical NTFET device.

Following the deposition of starch onto the FET—achieved by soaking the silicon wafer in a 5% aqueous starch solution—the  $I/V_g$  curve is shifted (Figure 3b) by approximately 2 V toward more negative gate voltages.<sup>16</sup> The direction of the shift equates with electron doping of the nanotube channel by the polysaccharide. Similar doping effects have been observed when carbon nanotube FET devices were exposed to NH<sub>3</sub> gas,<sup>12b</sup> to amines,<sup>11d</sup> poly(ethylene imine) (PEI),<sup>11c</sup> and proteins.<sup>13a</sup> However, the magnitude of the shift is smaller in the case of the starch-treated devices. For example, full coverage of the nanotube channel by PEI leads to an  $I/V_g$  shift of the order of 10 V, a magnitude which is five times larger than when the full coverage is with starch. This observation probably reflects the difference<sup>17</sup> between the electron-donating abilities of the hydroxyl groups and ether functions in starch, as opposed to the amino groups present in PEI.

If, after the enzyme-catalyzed reaction has been performed on the starch-functionalized device, it is washed with buffer, the  $I/V_g$  device characteristics recover almost completely (Figure 3c) to the trace recorded before the starch deposition.<sup>18</sup> This observation indicates that, during the enzyme-catalyzed reaction, nearly all the starch deposits on the surface of the nanotube device are hydrolyzed to glucose which is washed off by the buffer prior to the electronic measurements. Two control experiments were carried out to confirm these results. First of all, (i) the starch-functionalized chip was rinsed with buffer to find out if this solution alone can wash away the starch deposited on the device. After rinsing with the buffer solution, the  $I/V_g$  characteristics

(16) Since these deposition conditions are the same (ref 6), we can assume similar thicknesses for the starch layer to those measured by AFM on clean Si wafers, i.e., 30–100 nm uneven deposit. Moreover, since the starch deposit cannot interfere physically with the NTFET integrated circuit, only a charge-transfer interaction involving the starch is expected.

(17) Nitrogen is not as electronegative as oxygen, and amines have a greater tendency to react with a proton than do alcohols and ethers, viz., alkylxonium ions are more acidic than alkylammonium ions. Quantitatively, this difference can be expressed in the corresponding  $pK_a$  values, of primary < tertiary < secondary ethylamines ( $\text{EtNH}_3^+ = 10.64$ ,  $\text{Et}_3\text{NH}^+ = 10.75$ ,  $\text{Et}_2\text{NH}_2^+ = 10.94$ ) as compared to those of diethyl ether and ethanol ( $\text{Et}_2\text{OH}^+ = -3.6$ ,  $\text{EtOH}_2^+ = -2.4$ ).

(18) Electronic measurements, such as  $I/V_g$  characteristics and time-dependent transconductance measurements, can be conducted in a buffer using a liquid gate. See ref 13e. The real time detection of enzymatic hydrolysis of starch in the buffer is under investigation at present.

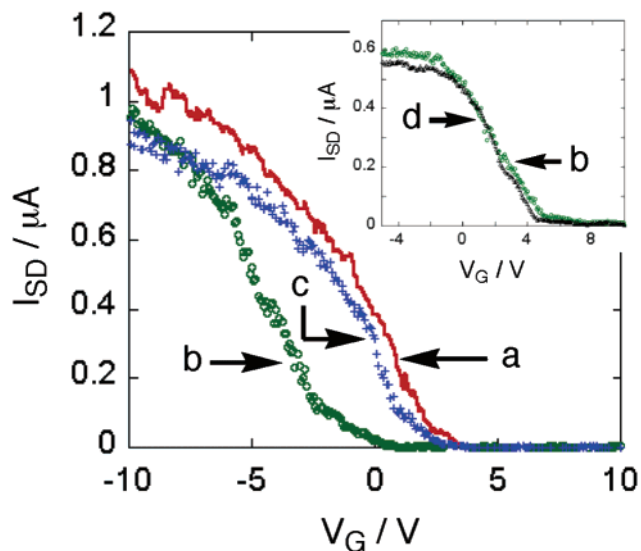


**Figure 3.** NTFET device characteristics in the form of  $I_{SD}/V_g$  curves measured from +10 to −10 V gate voltage with +0.6 V bias voltage (a) before and (b) after starch deposition (see caption to Figure 1), as well as (c) after hydrolysis with AMG. Inset shows a control experiment on a similar NTFET device ( $V_{SD} = +1$  V) where the starch-coated device (b) was exposed to buffer solution (no enzyme) resulted in (d) no change in the device characteristics.

are similar to those observed before rinsing, leading to the conclusion that the starch is not removed by the buffer alone. This observation is in good agreement with the conclusions (Figure 1b) we drew on the basis of the AFM studies. A second control experiment (ii) involved deposition of an enzyme solution onto the “bare” device, i.e., nanotube FETs without any starch deposition having been tried on them. Although the  $I/V_g$  characteristics display increased hysteresis, most likely as a consequence of mobile ions close to the conducting channel,<sup>11i</sup> no significant shift in the  $I/V_g$  curve is observed. This result provides evidence that the enzyme alone does not lead to significant charge transfer to the nanotube channel.

Thus, we have demonstrated the electronic detection of the enzymatic hydrolysis of starch using carbon nanotube-based FETs.<sup>18</sup> The process was also followed by direct imaging. The results of the experiments reported in this communication pave the way for using electronic detection technology in the study of enzyme-catalyzed reactions.

**Acknowledgment.** We thank the technical staff at Nanomix for their assistance with device fabrication and measurements. We also thank the National Center for Electron Microscopy at Lawrence Berkeley National Laboratory for making this facility available to us. The research was supported partially by NSF SBIR (NSF-0319991) and by the Director, Office of Science, Office of Basic Energy Sciences, of the U.S. Department of Energy under Contract No. DE-AC03-76SF00098.

OL0495826